# Enantioselective Homogeneous Catalysis and the "3,5-Dialkyl Meta-Effect". MeO−BIPHEP Complexes Related to Heck, Allylic Alkylation, and Hydrogenation Chemistry

**Gerald Trabesinger,[†] Alberto Albinati,[‡] Nantko Feiken,[†] Roland W. Kunz,[§] Paul S. Pregosin,*[,†] and Matthias Tschoerner[†]**

*Contribution from the Laboratorium für Anorganische Chemie, ETH Zentrum, 8092 Zürich, Switzerland, Organische Chemie, Universität Zürich, 8057 Zürich, Switzerland, and Chemical Pharmacy, University of Milan, I-20131 Milan, Italy*

*Received December 23, 1996. Revised Manuscript Received April 24, 1997*[⊗]

**Abstract:** The enantioselectivities arising from a Pd-catalyzed Heck reaction (>98% ee) and an allylic alkylation (>90% ee) using a 3,5-di-*tert*-butyl-MeO−BIPHEP chiral auxiliary (**1**) are reported. Higher ee's are observed with the 3,5-dialkyl substituents than with the unsubstituted parent MeO−BIPHEP. It is proposed that the observed dialkyl "meta-effect", on enantioselectivity, is the combined result of a more rigid and slightly larger chiral pocket and that this effect will have some generality in homogeneous catalysis. Detailed NMR studies on the allyl complex [Pd(PhCHCHCHPh)(**1**)]$PF_6$ (**5**), and the model hydrogenation catalyst [RuH(cymene)(**1**)]$BF_4$ (**6**), reveal restricted rotation about several of the P−C(ipso) bonds of the phosphorus substituents containing the 3,5-di-*tert*-butyl groups. The X-ray structure of **6** reveals that the cymene ligand is not symmetrically bound to the Ru atom. This observation is interpreted as an expression of the chiral pocket of **1**. MM3* calculations on **6** support the NMR findings and reproduce the X-ray results.

## Introduction

Enantioselective homogeneous catalysis with late transition metals is enjoying increasing application in organic synthesis, with hydrogenation, allylic alkylation, and Heck chemistry among the most successful reactions.[1] Although the necessary difference in activation energy, $\Delta\Delta G^{\ddagger}$, to achieve an enantiomeric excess (ee) of >90% is modest, <3 kcal/mol, an increasing number of chiral auxiliaries are capable of accomplishing this task in a variety of transformations.[2]

We have recently become involved with the bis(3,5-di-*tert*-butyl)-substituted chiral bidentate phosphine MeO−BIPHEP **1**,

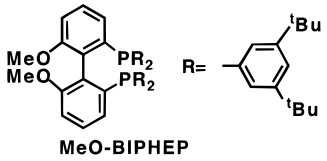


MeO-BIPHEP

**1**

originally prepared by Schmid and co-workers.[3] Ru complexes of **1** find practical application in that they afford >95% ee's in the enantioselective hydrogenation of a prochiral pyrone.[3] In terms of the relative ee, the 3,5-di-*tert*-butyl analog is at least 7% better than the parent unsubstituted derivative.[3]

The Ru(II) chemistry of **1** has proven to be both fruitful and novel. Starting from $Ru(OAc)_2$(**1**), one can isolate a stable "stripped-down" cationic five-coordinate hydrido−bissolvento complex, [RuH(*i*-PrOH)$_2$(**1**)]$BF_4$ (**2**), from the hydrogenation reaction mixture.[4] This is the first well-characterized chiral five-coordinate bis(phosphine)ruthenium hydride complex stable as a solvento complex. Compound **2** is also an effective hydrogenation precursor. Moreover, ligand **1** is capable of serving as a *six*-electron donor[5] in that one of the biaryl double bonds can coordinate to Ru(II) as shown in the $\eta^5$-$C_8H_{11}$–pentadienyl complex **3**.

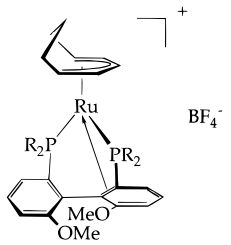


**4**

**3** R = 3,5-di-t-butyl phenyl, **a** or i-Pr, **b**

We report here (a) new catalytic results using **1** in both the Pd-catalyzed enantioselective Heck and allylic alkylation reactions and (b) new solid-state and solution structural chemistry for Ru and Pd complexes based on **1**. Using the results from these studies, together with new MM3* calculations, allows a

[†] ETH Zentrum.
[‡] University of Milan.
[§] Universität Zürich.
[⊗] Abstract published in *Advance ACS Abstracts,* June 1, 1997.

(1) Trost, B. M. ; van Vranken, D. L. *Chem. Rev.* **1996**, *96*, 395. Genet, J. P.; *Acros. Org. Acta* **1995**, *1*, 4. Tanner, D. *Angew. Chem., Int. Ed. Engl.* **1994**, *106*, 625. Brown, J. M. *Chem. Soc. Rev.* **1993**, 25. Kitamura, M.; Noyori, R. In *Modern Synthetic Methods*; Scheffold, R., Ed.; Springer-Verlag: New York, 1989; 5, p 116.

(2) Togni. A.; Venanzi, L. M. *Angew. Chem.* **1994**, *33*, 497. Hayashi, T. In *Catalytic Asymmetry Synthesis*; Ojima, I., Ed.; VCH Publishers, Inc.: New York, 1993; p 325.

(3) Schmid, R.; Broger, E. A.; Cereghetti, M.; Crameri, Y.; Foricher, J.; Lalonde M.; Mueller, R. K.; Scalone, M.; Schoettel, G.; Zutter, U. *Pure Appl. Chem.* **1996**, *68*, 131.

(4) Currao, A.; Feiken, N.; Macchioni, A.; Nesper, R.; Pregosin P. S.; Trabesinger, G. *Helv. Chim. Acta* **1996**, *79*, 1587.

(5) Feiken, N.; Pregosin, P. S.; Trabesinger, G. *Organometallics* **1997**, *16*, 537−543.

S0002-7863(96)04406-X CCC: $14.00 

rationalization of the higher ee's observed with **1** and with a number of different chiral bis(3,5-dialkylaryl)phosphine ligands.

## Results

**Catalytic Results.** The enantioselective Heck reaction,[6,8] involving dihydrofuran and phenyl triflate, described by Hayashi,[6] proceeds slowly with **1** as auxiliary, but in very high ee, as shown in eq 1. An analogous experiment with the

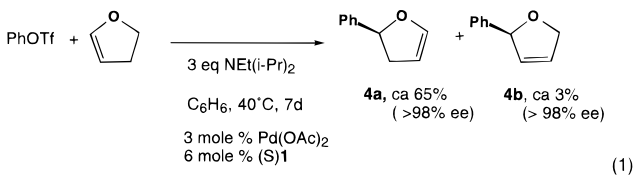


(1)

unsubstituted parent MeO−BIPHEP (i.e, no meta-substituent) afforded **4a** in 84% ee (71% chemical yield). As in the Ru chemistry, noted above, the 3,5-di-*tert*-butyl-MeO−BIPHEP analog is superior in terms of enantioselectivity. For the same reaction, Pfaltz and co-workers[8] have achieved the same ee using an oxazoline-based chiral auxiliary. Interestingly, Hayashi finds that **4b** and not **4a** is the major product using (*R*)-BINAP as auxiliary.

We find both the chemical yields, and to a lesser extent the ee's for this Heck chemistry, to be sensitive to the nature of the base and solvent. The observed ee using **1** plus $Pd(OAc)_2$ with $Ag_2CO_3$ in DMF was 90%; however, the chemical yield of **4a** was only 2.1%. Using THF as solvent, with $NEt(i\text{-}Pr)_2$ as base, at 70 °C for 7 d, also gives ca. 98% ee, but again low yields (34% and 3% for **4a** and **4b**, respectively). Use of the standard Pd(0) reagent $Pd_2$(dibenzylidene acetone)$_3$·$C_6H_6$ at 70 °C for 7 d in benzene affords yields of ca. 44% and 2% for **4a** and **4b**, respectively, with the ee's remaining ca. 98%. Hayashi and co-workers[6] have previously reported a base dependency.[6]

The enantioselective allylic alkylation of the classical 1,3-diphenyl acetate substrate[13] (eq 2) was carried out using the

$$\mathrm{PhCH(OAc)CH{=}CHPh} + \mathrm{CHR_2^-} \rightarrow \mathrm{PhC^*H(CHR_2)CH{=}CHPh} + \mathrm{OAc^-}\ (\mathrm{R} = \mathrm{CO_2Me}) \quad (2)$$

1,3-diphenylallyl complex [Pd(PhCHCHCHPh)(**1**)]$PF_6$ (**5**) as catalyst precursor. We find a 70% yield of product with an ee of ca. 91%. The analogous control experiment with the parent MeO−BIPHEP afforded a ca. 87% ee[14] so that again **1** is superior, if only slightly.

**NMR Spectroscopy of 5.** We have recently determined the 3-D solution structures for a series of chiral $\pi$-allyl complexes of Pd(II).[14a−17] For JOSIPHOS, CHIRAPHOS, BINAP, and BIPHEP type complexes one can define the shape of the phenyl chiral array, using NOESY methods. The steric interactions between these phenyls and, e.g., a coordinated 1,3-diphenylallyl substrate, are pin-pointed via intramolecular NOEs. As a consequence of these short contacts this structural $\pi$-allyl chemistry is accompanied by specific $\eta^3-\eta^1-\eta^3$-isomerization processes.[16] Given the detail available from these NMR studies we have undertaken a similar set of measurements on **5**.

The $^{31}$P NMR spectrum of the diphenylallyl complex **5** reveals two components, **5a** and **5b**, in the ratio ca. 1.7:1, which,

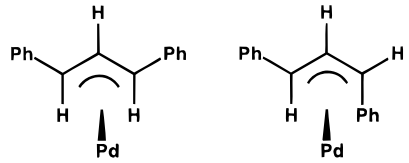


syn/syn isomer **5a** syn/anti isomer **5b**

with the help of $^1$H and $^{13}$C NMR measurements, can be assigned to syn/syn and syn/anti isomers. Obviously, the observed ee for the allylation in eq 2 does not correspond to the measured ground-state populations of the two diastereomers. The same can be said for the ee and populations involving the allylic alkylation chemistry of the parent MeO−BIPHEP auxiliary.[14a]

The room temperature $^1$H spectrum for **5** shows that several of the aromatic and *tert*-butyl proton signals are broad. A series of variable temperature and 2-D NMR experiments lead to the assignment of the pertinent resonances (see Table 1 for details) and reveals restricted rotation for the $\alpha$, $\beta$, and $\gamma$-phenyl rings of **5a**, *at room temperature* (see Figure 1a). At 193 K all four

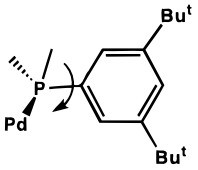


rings are frozen, and Figure 1b shows the 16 nonequivalent *tert*-butyl signals (8 each for **5a** and **5b**). The 20 nonequivalent ortho-ring protons are readily detected via a 2-D $^{31}$P,$^1$H-correlation (see Figure 2). The variable temperature studies reveal that **5b** has two rings frozen at ambient temperature (the four unlabeled sharp singlets in the top half of the figure). There is no observable exchange between **5a** and **5b** at ambient temperature in $CD_2Cl_2$. In uncoordinated **1** there is relatively fast rotation around these P−C(ipso) bonds at ambient temperature.

The $^{13}$C chemical shifts of the allyl termini in **5a** (102.2 and 83.8 ppm) and **5b** (98.1 and 90.7 ppm) fall in the expected range.[14a,15,16] However, the intramolecular differences, $\Delta^{13}$C,

(6) Ozawa, F.; Kubo. A.; Matsumoto, Y.; Hayashi, T.; Nishioka, I.; Yanagi, K.; Moriguchi, K *Organometallics* **1993**, *12*, 4188. In this paper, **4b** and not **4a** is the major product.

(7) Cabri, W.; Candiani, I. *Acc. Chem. Res*. **1995**, *28*, 2. Brown, J. M.; Perez-Torrente, J.; Alcock, N.; Clase, H. J. *Organometallics* **1995**, *14*, 207.

(8) Pfaltz, A. *Acta Chem. Scand.* **1996**, *50*, 189.

(9) Reiser, O. *Angew. Chem.* **1993**, *105*, 576.

(10) von Matt. P.; Lloyd-Jones, G. C.; Minidis, A. B. E.; Pfaltz, A.; Macko, L.; Neuburger, M.; Zehnder, M.; Rüegger, H, Pregosin, P. S. *Helv. Chim. Acta* **1995**, *78*, 265.

(11) Rieck, H.; Helmchen, G. *Angew. Chem.* **1995**, *107*, 2881. Knühl, G.; Sennhenn, P.; Helmchen, G. *J. Chem. Soc., Chem. Commun.* **1995**, 1845. Knühl, G.; Sennhenn, P.; Helmchen, G. *J. Chem. Soc., Chem. Commun.* . **1995**, 1845.

(12) (a) Mackenzie, P. B.; Whelan, J.; Bosnich, B. *J. Am. Chem. Soc.* **1985**, *107*, 2046. (b) Auburn, P. R.; Mackenzie, P. B.; Bosnich, B. *J. Am. Chem. Soc*. **1985**, *107*, 2033. (c) Andersson, P. G.; Harden, A.; Tanner, D.; Norrby, P. O. *Chem. Eur. J*. **1995**, *1*, 12.

(13) Trost, B. M. *Acc. Chem. Res.* **1980**, *13*, 385.

(14) (a) Barbaro, P. Pregosin, P. S.; Salzmann, R.; Albinati, A.; Kunz, R., W. *Organometallics* **1995**, *14*, 5160. (b) Bolm, C.; Kaufmann, D.; Gessler, S.; Harms, K. *J. Organomet. Chem.* **1995**, *502*, 47.

(15) (a) Barbaro, P.; Currao, A.; Herrmann, J.; Nesper, R.; Pregosin, P. S.; Salzmann. *Organometallics* **1996**, *15*, 1879. (b) Albinati, A.; Pregosin, P. S.; Wick, K. *Organometallics* **1996**, *15*, 2419. (c) Herrmann, J.; Pregosin, P. S.; Salzmann, R.; Albinati, A. *Organometallics* **1995**, *14*, 3311. (d) Pregosin, P. S.; Rüegger, H.; Salzmann, R.; Albinati, A.; Lianza, F.; Kunz, R. W. *Organometallics* **1994**, *13*, 83. (e) Pregosin, P. S.; Rüegger, H.; Salzmann, R.; Albinati, A.; Lianza, F.; Kunz, R. W. *Organometallics* **1994**, *13*, 5040.

(16) Pregosin, P. S.; Salzmann, R. *Coord. Chem. Rev*. **1996**, *155*, 35.

(17) (a) Togni, A.; Burckhardt, U.; Gramlich, V.; Pregosin, P.; Salzmann, R. *J. Am. Chem. Soc*. **1996**, *118*, 1031. (b) Pregosin, P. S.; Salzmann, R.; Togni, A. *Organometallics* **1995**, *14*, 842. (c) Breutel, C.; Pregosin, P. S.; Salzmann, R.; Togni, A. *J. Am. Chem. Soc*. **1994**, *116*, 4067.

**Table 1.** $^{1}$H-, $^{13}$C-, and $^{31}$P-NMR Data[a] for **5a** and **5b**

| | **5a** (syn/syn) | | **5b** (syn/anti) | |
|---|---|---|---|---|
| | $^{1}$H | $^{13}$C | $^{1}$H | $^{13}$C |
| 3 | 6.22 | 114.0 | 6.25 | |
| 4 | 6.79 | | 6.88 | |
| 5 | 6.07 | 123.9 | 6.53 | |
| 7 | 3.17 | 57.1 | 3.15 | 56.8 |
| 3′ | 6.36 | | 6.37 | |
| 4′ | 7.17 | | 7.06 | |
| 5′ | 7.03 | | 7.17 | |
| 7′ | 3.23 | 57.0 | 3.19 | 57.1 |
| o-α | 7.38 | | 7.47 | |
| o-α | 6.44 | | 6.45 | |
| *t*-α | 1.43 | | 1.38 | |
| *t*-α | 0.98 | | 0.97 | |
| p-α | 7.33 | | 7.52 | |
| o-*β* | 7.48 | | 6.70 | |
| o-*β* | 6.93 | | 6.90 | |
| *t*-*β* | 1.33 | | 1.06 | |
| *t*-*β* | 1.20 | | 1.26 | |
| p-*β* | 7.53 | | 7.33 | |
| o-*γ* | 6.72 | | 6.92 | |
| o-*γ* | 6.55 | | 6.38 | |
| *t*-*γ* | 1.06 | | 1.16 | |
| *t*-*γ* | 1.09 | | | |
| p-*γ* | 7.26 | | | |
| o-*δ* | 6.41 | | 7.13 | |
| o-*δ* | 7.76 | | 7.79 | |
| *t*-*δ* | 1.06 | | 1.15 | |
| *t*-*δ* | 1.09 | | 1.45 | |
| p-*δ* | 7.61 | | 7.52 | |
| 8 | 5.85 | 102.1 | | |
| 9 | 6.32 | 109.6 | | |
| 10 | 3.93 | 83.8 | | |
| $P_A$ | 29.7 | | 24.5 | |
| $P_B$ | 25.7 | | 20.9 | |
| $^{2}J(P_A-P_B)$ | 75.5 | | 71.0 | |

[a] Chemical shifts in parts per million, *J* values in hertz; 193 K, $CD_2Cl_2$. [b] o = phosphine ortho protons, *t* = *t*-Bu methyl groups, p = phosphine para protons. See Chart 1.

between the allyl termini in **5a** (14.4 ppm) and **5b** (7.4 ppm) are suggestive. Assuming (a) $\Delta^{13}$C is due to steric effects (and specifically, the D,F-ring-stacking indicated below,

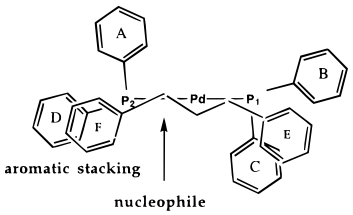


Fragment of the chiral array for an S (-) MeO-BIPHEP

superimposed on a coordinated 1,3-diphenyl allyl

and described previously[14a]) and (b) that the highest frequency carbon, shown by the arrow, will be attacked preferentially as it is not as strongly bound and thus more electrophilic, then one can successfully predict the chirality of the product. This rationale requires that the two isomers be in equilibrium; i.e., **5a** reacts preferentially and then **5b** is drawn off via the equilibrium. This is reasonable as the observed kinetics are quite slow.[12a,b]

Unfortunately, substantial signal overlap together with developing slow rotation around the allyl C(allyl)−C(phenyl) carbon−carbon bonds hindered a quantitative analysis of the rotational barriers; however, the spectroscopy was somewhat simpler for the arene Ru complex **6**.

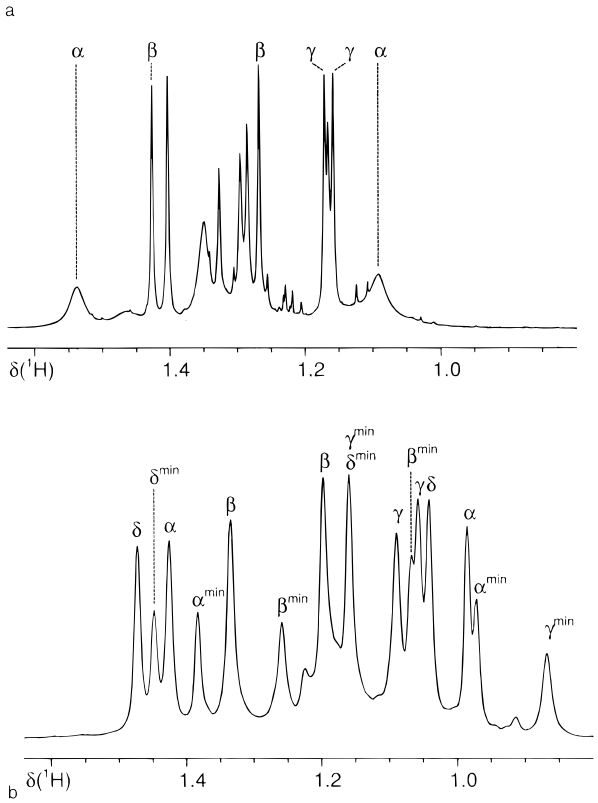


**Figure 1.** (a) *tert*-Butyl region of the $^{1}$H-spectrum for **5** at ambient temperature (top). (b) Spectrum at 193 K (bottom). The low-temperature spectrum reveals eight nonequivalent *tert*-butyl resonances in both isomers due to hindered rotation around the P−C(ipso) axes. The assignment can be made via a series of variable temperature measurements together with NOE results ($CD_2Cl_2$, 500 MHz).

**X-ray Structure of [RuH(*p*-cymene)(1)]$BF_4$ (6).** Given the effectiveness of the ruthenium hydrido complex **1** in the enantioselective hydrogenation,[3] we prepared the model cymene complex **6** as shown in eq 3. Given the dearth of structures for

$$\mathrm{Ru(OAc)_2}(\mathbf{1}) + \text{cymene} \xrightarrow[\mathrm{H_2\ (1\ atm),\ CH_2Cl_2}]{2\mathrm{HBF_4}} [\mathrm{RuH(cymene)}(\mathbf{1})]\mathrm{BF_4}\ (\mathbf{6}) + 2\ \mathrm{HOAc} + \mathrm{HBF_4} \quad (3)$$

chiral hydridoruthenium compounds of chelating phosphines, the solid-state structure of complex **6** was determined by X-ray diffraction methods.

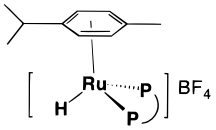


**6**, PP = **1**

An ORTEP plot for the cation is given in Figure 3. The immediate coordination sphere consists of the six *π*-complexed arene carbons and the two P atoms of the chiral bidentate MeO−BIPHEP. There is a THF solvent molecule in the unit cell. The hydride was located by minimizing the ligand repulsion (see the Experimental Section). The space in which the hydride sits is relatively large, and the associated bond lengths and bond angles fall in the expected ranges. As in the structure of **2**, we note that coordinated **1** takes up a substantial amount of space around the metal. Table 2 contains a list of selected bond lengths and bond angles for **6** and Table 3, experimental parameters.

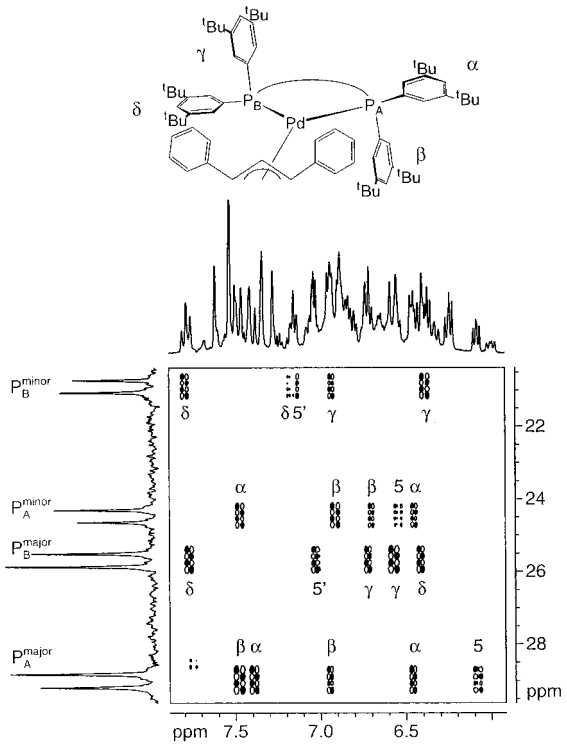


**Figure 2.** $^{31}P,^{1}H$-correlation spectrum of **5a** and **5b** showing the aromatic region. Five correlation peaks are visible for each $^{31}P$-spin (20 for the two diastereomers): one each due to the biaryl protons, 5 and 5′, and four from the nonequivalent orthoprotons. Once these are assigned, NOE results can be used for detailed structural work ($CD_2Cl_2$, 500 MHz).

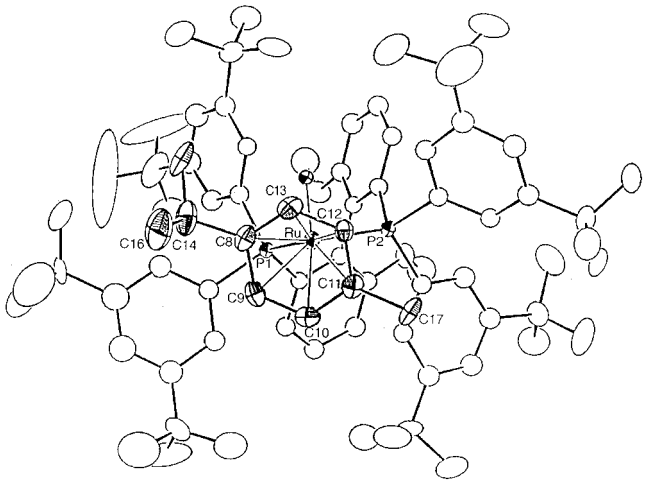


**Figure 3.** ORTEP plot for the cation of **6**. The shaded ellipsoids show the coordinated arene (C8−C17), plus the Ru, P1, P2, and hydride atoms.

The Ru−P distances in **6** are modest in length, 2.291(2) and 2.326(2) Å. Cymene complexes of ruthenium are well-known catalyst precursors, and the structures of several phosphine-containing complexes have been determined. Zanetti et al.[18] reported structural details for [RuCl(cymene)(JOSIPHOS)]($PF_6$) (**7**), which contains a large ferrocene-based chiral bidentate phosphine. They find longer Ru−P separations of 2.368(2) and 2.390(2) Å. In the cationic mono-phosphine−hydride complex [RuH(styrene)(cymene)($PPh_3$)]$^+$ (**8**) Faller and Chase[19] report the Ru−P distance to be 2.297(7) Å. Consequently, although

**Table 2.** Selected Bond Lengths (Å) and Bond Angles (deg) for **6**

| | | | |
|---|---|---|---|
| Ru−P2 | 2.291(2) | Ru−P1 | 2.326(2) |
| Ru−C8 | 2.298(7) | Ru- C9 | 2.306(7) |
| Ru−C10 | 2.333(7) | Ru−C11 | 2.313(7) |
| Ru−C12 | 2.260(7) | Ru−C13 | 2.251(7) |
| Ru−Hyd | 1.66(9) | | |
| C8−C9 | 1.442(11) | C8−C13 | 1.390(11) |
| C8−C14 | 1.527(11) | C9−C10 | 1.402(10) |
| C10−C11 | 1.402(10) | C11−C12 | 1.420(10) |
| C12−C13 | 1.421(10) | C11−C17 | 1.532(10) |
| P1−Ru−P2 | 91.07(6) | P2−Ru−C11 | 94.9(2) |
| P2−Ru−C10 | 116.3(2) | P2−Ru−C9 | 150.5(2) |
| P2−Ru−C8 | 162.8(2) | P2−Ru−C13 | 127.3(2) |
| P2−Ru−C12 | 99.3(2) | P1−Ru−C11 | 144.7(2) |
| P1−Ru−C10 | 112.6(2) | P1−Ru−C9 | 95.9(2) |
| P1−Ru−C8 | 104.4(2) | P1−Ru−C13 | 133.9(2) |
| P1−Ru−C12 | 169.5(2) | P2−Ru−Hyd | 82(3) |
| P1−Ru−Hyd | 86(3) | | |

**Table 3.** Experimental Data for the X-ray Diffraction Study of [RuH(*p*-Cymene)(**1**)]$BF_4$·$C_4H_8O$ (**6**)

| | |
|---|---|
| formula | $C_{84}H_{118}BF_4O_3P_2Ru$ |
| mol wt | 1425.70 |
| crystal dim, mm | 0.50 × 0.40 × 0.30 |
| data collectn *T*, K | 180(1) |
| cryst syst | orthorombic |
| space group | $P2_12_12_1$ |
| *a*, Å | 15.856(3) |
| *b*, Å | 20.643(2) |
| *c*, Å | 24.396(3) |
| *V*, Å$^3$ | 7985(2) |
| *Z* | 4 |
| $\rho$(calcd), g cm$^{-3}$ | 1.186 |
| $\mu$, cm$^{-1}$ | 2.834 |
| radiation | Mo Kα (graphite monochromated, $\lambda$ = 0.710 69 Å) |
| no. of indep data collected | 7605 |
| no. of obsd reflns ($n_o$) ($\|F_o\| > 3.0\sigma(\|F\|)$) | 6193 |
| transmission coeff. | 0.9982−0.9371 |
| no. of params refined ($n_v$) | 650 |
| $R^a$ | 0.0547 |
| $R_w{}^a$ | 0.0691 |
| GOF | 3.092 |

$^a$ $R = \sum(|F_o - (1/k)F_c|)/\sum|F_o|$. $R_w = [\sum_w(F_o - (1/k)F_c)^2/\sum_w|F_o|^2]^{1/2}$, where $w = [\sigma^2(F_o)]^{-1}$. $\sigma(F_o) = [\sigma^2(F_o{}^2) + f^4(F_o{}^2)]^{1/2}/2F_o$. $f = 0.03$.

**1** is a relatively large ligand, there is no unusual lengthening of the metal−phosphorus bond in **6**. The P−Ru−P angle, 91.07-(6)°, is normal.

On the other hand, the observed Ru−C(cymene) distances in **6**, ca. 2.25−2.33 Å, are all relatively long. These separations are in agreement with the analogous distances in **7**, but in contrast to the ca. 2.18−2.24 Å range of Ru−C(cymene) values found in complexes of pyrazolylmethane and pyrazolyl borate,[20] among others.[21−24] Close inspection of the Ru−C(cymene) bond lengths in **6** reveals that the distances Ru−C12 and Ru−C13 are shorter than Ru−C9 and Ru−C10, suggesting a "tilted" mode of coordination. The aromatic C−C bond lengths within the arene, ca. 1.39−1.44 Å are as expected.[19−28]

(18) Zanetti, N. C.; Spindler, F.; Spencer, J.; Togni, A.; Rihs, G. *Organometallics* **1996**, *15*, 860.
(19) Faller, J. W. Chase, K. J. *Organometallics* **1995**, *14*, 1592.
(20) Bhambri, S.; Tocher, D. A. *Polyhedron* **1996**, *15*, 2763.
(21) Yamamoto, Y.; Sato, R.; Matsuo, F.; Sudoh, C.; Igoshi, T. *Inorg. Chem.* **1996**, *35*, 2329.
(22) Tocher, D. A.; Gould, R. O.; Stephenson, T. A.; Bennett, M. A.; Ennett, J. P.; Matheson, T. W.; Sawer, L.; Shah, V. K. *J. Chem. Soc., Dalton Trans.* **1983**, 1571.
(23) Porter, L. C.; Polam, J. R.; Bodige, S. *Inorg. Chem.* **1995**, *34*, 998.
(24) ; Bennett, M. A.; Goh, L. Y.; Willis, A. C. *J. Am. Chem. Soc.* **1996**, *118*, 4984. Bennett, M. A.; Matheson, T. W.; Robertson, G. B.; Smith, A. K.; Tucker, P. A. *Inorg. Chem.* **1981**, *20*, 2353.
(25) Hashiguchi, S.; Fujii, A.; Takehara, J.; Ikariya, T.; Noyori, R. *J. Am. Chem. Soc.* **1995**, *117*, 7562.

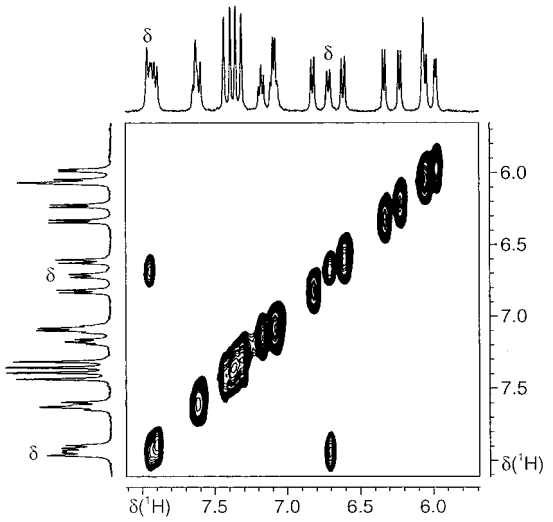


**Figure 4.** Section of the 2-D NOESY for **6** at 193 K showing that two of the ortho protons of the $\delta$ ring are in slow exchange ($CD_2Cl_2$, 500 MHz).

One of the most interesting features of the structure concerns the ca. 45° twist made by the arene C11−C17 vector, relative to a symmetric position defined by the metal and the two P atoms. Obviously, the chiral array is enforcing a steric preference upon this complexed arene.

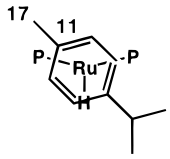


**Solution Structure for RuH(*p*-cymene)(1) (6).** We have previously reported[5] a set of variable temperature $^1$H-spectra demonstrating that **6** is dynamic on the NMR time scale. Analysis of these spectra reveals the same type of restricted rotation about the P−C(ipso) bonds, noted above in **5**. All of the P−aryl rotations are restricted at 193 K; however, the $\delta$-ring is rotating just fast enough so that exchange cross-peaks between its two ortho protons are visible (see Figure 4). The eight nonequivalent ortho protons of **1** (plus the *o*-binaphthyl proton) can be located and eventually assigned starting with a $^{31}$P,$^1$H-correlation, as shown in Figure 5. The four relatively sharp singlets at ca. 7.35 ppm, in Figure 5, represent the four nonequivalent para protons of the rings. At ambient temperature only one ring, $\beta$, is rotating slowly (see Chart 1) in contrast to **5**. The activation barriers (kJ/mol), determined by line shape analyses of the *tert*-butyl signals, for rotation about the three relatively unhindered P−C bonds are 50.0 ($\gamma$), 42.4 ($\alpha$), and 36.2 ($\delta$) with the two smallest values associated with the two pseudo-equatorial substituents (see the Experimental Section for details). In the absence of 2-(and/or 6) substitution, P−phenyl substituents in complexes of bidentate chiral phosphines normally rotate freely.[29] Therefore, our data for **5** and **6** represent the first report of such restricted rotation, and indicate a well-defined, relatively rigid chiral pocket.

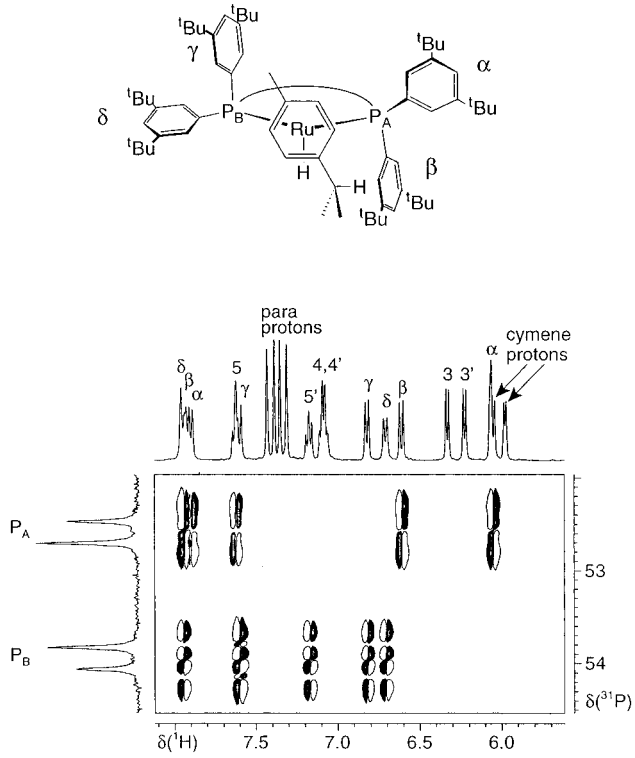


**Figure 5.** $^{31}$P,$^1$H-correlation spectrum of **6** showing the aromatic region. Ten correlation peaks are visible: one each due to the biaryl protons, 5 and 5′, and eight from the nonequivalent ortho protons. This is an unusually well-resolved example and also demonstrates the four nonequivalent para protons as singlets (193 K, $CD_2Cl_2$, 500 MHz).

**Chart 1**

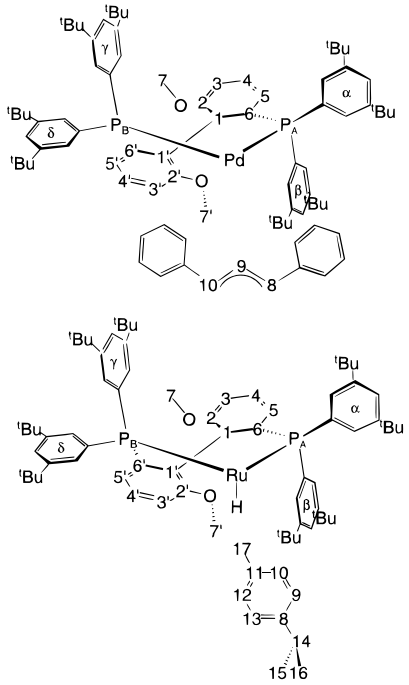


The remaining proton signals can be assigned by classical 2-D measurements, and details of these can be found in Table 4. Figure 6 shows that there is a selective NOE from the Ru−H resonance to one of the two cymene aromatic protons ortho to the methyl group (and also a strong NOE to one ortho to the *i*-Pr). This confirms that the Me−C vector of the cymene is rotated relative to the P−Ru−P plane, as found in the solid-state structure. The rotation brings one of these two protons

(26) Mashima, K.; Kusano, K.; Ohta, T.; Noyori, R. Takaya, H. *J. Chem. Soc., Chem. Commun.* **1989**, 1208.

(27) Bank, J.; Gevert, O.; Wolfsberger, W.; Werner, H. *Organometallics* **1995**, *14*, 4972.

(28) Bhambri, S.; Tocher, D. A. *J. Organomet. Chem.* **1996**, *507*, 291.

(29) There are indications that Binap−allyl complexes show the same restricted rotation, although the activation energy is somewhat lower; i.e., the rotation is not yet slow at ambient temperature. See: Rüegger, H.; Kunz, R. W.; Ammann, C. J.; Pregosin, P. S. *Magn. Reson. Chem.* **1992**, *29*, 197.

**Table 4.** NMR Data for **6**[a]

| $^1$H ($^{13}$C) | | | |
|---|---|---|---|
| 3 | 6.33 | 4 | 7.08 |
| 5 | 7.61 | 7 | 3.12 |
| 3′ | 6.23 | 4′ | 7.09 |
| 5′ | 7.18 | 7′ | 2.97 |
| o-α | 7.90 | o-α | 6.05 |
| *t*-α | 1.48 | *t*-α | 0.91 |
| p-α | 7.35 | | |
| o-*β* | 7.95 | o-*β* | 6.61 |
| *t*-*β* | 1.24 | *t*-*β* | 0.96 |
| p-*β* | 7.31 | | |
| o-*γ* | 7.61 | o-*γ* | 6.82 |
| *t*-*γ* | 1.37 | *t*-*γ* | 1.09 |
| p-*γ* | 7.31 | | |
| o-*δ* | 7.95 | o-*δ* | 6.71 |
| *t*-*δ* | 1.45 | *t*-*δ* | 1.04 |
| p-*δ* | 7.39 | | |
| 9 | 3.35 (107.3) | 10 | 6.06 (92.7) |
| 12 | 2.76 (94.7) | 13 | 5.98 (89.4) |
| 14 | 1.56 | 15 | 1.07 |
| 16 | 0.71 | 17 | 1.61 |
| hydride[b] | −9.80 | | |

[a] 193 K, $CD_2Cl_2$, o = ortho, *t* = t-Bu methyl group, p = para. See Chart 1. [b] $P_A = 52.6$, $P_B = 54.0$, $^2J(P_A-P_B) = 46$ Hz.

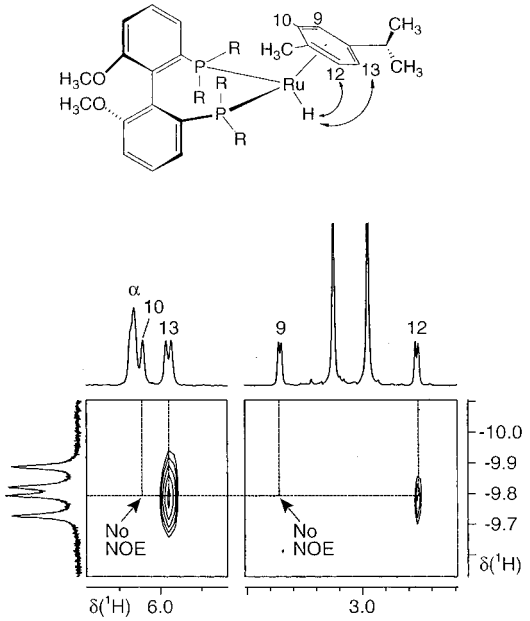


**Figure 6.** Section of the ROESY spectrum showing the hydride contacts to the aromatic cymene protons. The moderate H12 contact together with the strong H13 contact proves that the cymene is rotated as described in the text. Note that there are *no* contacts to H9 and H10 ($CD_2Cl_2$, 193 K, 500 MHz, carrier frequency set on −5.0 ppm).

much closer to the hydride, i.e.,

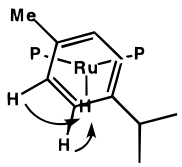


fragment showing the consequence of rotation in terms of the observed selective NOE to one proton ortho to the methyl group.

From the X-ray data one finds separations of 2.6(1) Å for Ru−H to H13 and 3.2(1) Å for Ru−H to H12, in reasonable agreement with the observed solution NOEs, given the uncertainty in the hydride position. The qualitative solution structure as determined by NOE methods is in agreement with the structure in the solid state.

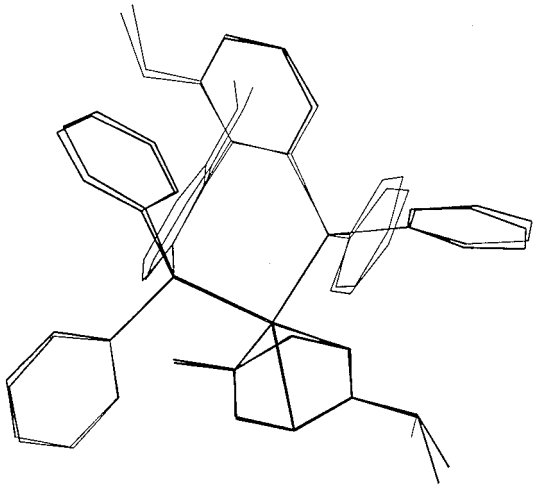

**Figure 7.** Superimposed calculated (MM3*) and X-ray experimental results for the backbone structure of **6**. The *tert*-butyl groups have been omitted for clarity. The two structures are seen to be closely related.

The coordinated cymene of **6** reveals several interesting chemical shifts: (a) The $^{13}$C resonances for the two cymene carbons ortho to the *i*-Pr group are separated by 17.8 ppm (107.2 and 89.4 ppm), with the former at unusually high frequency, on the basis of literature expectations.[24−28] We assume that this difference stems from the asymmetric bonding of the arene to the metal, as suggested by the X-ray data. The two carbons ortho to the methyl group are only 1.7 ppm apart. (b) The four aromatic cymene protons are quite different, with two of these at very low frequency, as shown:

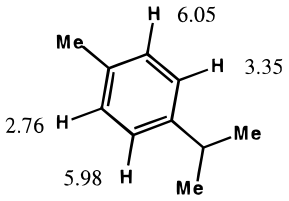


The protons at 2.76 and 3.35 ppm are shielded as a consequence of the local anisotropic effects of the equatorial phenyl substitutents[30] situated on the P atoms.

**MM3* Calculations.** Given the interesting structural features of **6**, we carried out MM3* calculations on three cationic complexes: [RuH(**1**)(cymene)]$^+$ (**6**), the unsubstituted MeO−BIPHEP parent analog, and the 3,5-dimethyl derivative, i.e., for **1** with R = H, $CH_3$, and $C(CH_3)_3$.

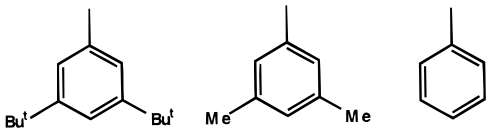


The immediate coordination sphere X-ray data for **6** were used as input parameters. Figure 7 shows part of the calculated structure of **6** superimposed on the solid-state result. Clearly the calculated structure is in good agreement (R = 0.065 Å) with the experimentally observed result, suggesting, as in previous studies, that the method is producing realistic results.

(30) Pretsch E.; Seibl. J.; Simon, W. *Strukturaufklärung organischer Verbindungen* Springer-Verlag: Berlin, 1986.

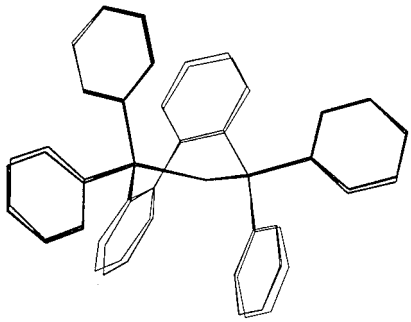

**Figure 8.** Superimposed calculated (MM3*) results for the BIPHEP backbone structures of the H-, Me-, and *t*-BuRu cations. The meta substitutents have been omitted for clarity. The three structures are seen to be closely related.

Figure 8 shows the calculated BIPHEP backbone structures for the three cations, again superimposed upon one another, to highlight potential differences. Inspection of this figure, plus analysis of various angular data, reveals that the structures of these three complexes are closely related; i.e., introduction of the meta substitutents does not change the basic structure.

The effect of arene rotation on structure was considered. Unexpectedly, the calculations suggest *four* relatively low energy possibilities for each of the three cations. For **6**, two of these have almost identical energies and might well be populated, whereas two are found somewhat higher in energy (ca. 16 and 27 kJ/mol above the minimum). If one defines an angle between the Ru−H and Me−C(ipso) vectors as $\phi$, then the two lowest

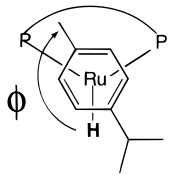


ϕ = -120˚ represents the X-ray result.

energy solutions for **6** have $\phi$ = ca. −120° (this is the lowest energy structure and corresponds to the X-ray and NMR result) and + 120° (ca. 1 kJ higher). The remaining structures have $\phi$ = −30° and +150°, with the latter at highest energy. Consequently, the observed positioning of the arene may not be general and moreover need not have much significance. Indeed, we have observed a second isomer in solution, at the ca. 5% level at low temperature, which might well be the second low-energy rotational isomer. The calculations also suggest that the two arene protons, H13 and H12, should be separated by ca. 2.3 and 3.0 Å, respectively, from the hydride, in good agreement with the NOE measurement shown in Figure 6.

For the dimethyl and parent complexes, the picture is qualitatively the same. The lowest energy rotamer always has $\phi$ = −120°, and the highest, with $\phi$ = +150°, is at least ca. 17 kJ/mol above the minimum energy; however, the relative energies of the remaining isomers vary.

The calculated rotational barriers about the four different P−phenyl substituents, for the three cations, are shown in Table 5. These are not (and are not expected to be) in agreement with the solution data. Solvent, ion-pairing, and counterion effects are likely to be considerable, so we take these numbers to have relative significance. Nevertheless, Table 5 shows, for **6**, that there are two groups of two, with the pseudoaxial rings having the highest barriers, in rough agreement with our solution observations. However, assigning the highest barrier to the $\gamma$-ring contradicts the solution observation for **6**. Further, the calculations predict that the difference in rotational barriers between pseudoaxial and pseudoequatorial rings will decrease on going from R = *tert*-butyl to R = Me.

**Table 5.** Approximate Rotational Barriers (kJ/mol) about the P−C(ipso) Phenyl Substituents As Calculated by MM3* [a]

| ring | H | Me | *t*-Bu (**6**) |
|---|---|---|---|
| α | 30 | 35 | 45 |
| $\beta$ | 50 | 50 | 110 |
| $\delta$ | 30 | 30 | 40 |
| $\gamma$ | 50 | 55 | 125 |

[a] $\beta$ and $\gamma$ are pseudoaxial and α and $\delta$ pseudoequatorial rings. The three complexes are $[RuH(\mathbf{1})(cymene)]^+$ (**6**), the unsubstituted MeO−BIPHEP parent analog, and the 3,5-dimethyl derivative; i.e., for **1** R = H, $CH_3$, and $C(CH_3)_3$.

The unexpectedly high barriers to rotation in **6** arise from the inability of the axial rings to rotate past the biaryl moiety. Since there is free rotation in uncoordinated **1** at ambient temperature, complexation to the transition metal compresses **1** somewhat. It is important to note that the closest contacts from the chiral auxiliary to the substrate (cymene in **6**, but 1,3-diphenylallyl in **5**) stem from the pseudoequatorial rings. For these rings, the calculations suggest a small but noticeable increase of ca. 5−10 kJ/mol in the rotational barrier, on going from R = H to R = *t*-Bu. Therefore, the entire chiral array becomes increasingly rigid, relative to the parent complex, with increasing size of the meta-substituents.

## Discussion

From the catalytic results in both the Heck reaction and the allylic alkylation, it is clear that the 3,5-di-*tert*-butyl substituents improve the enantioselectivity. A similar observation has been made by Schmid and co-workers[3] in the enantioselective hydrogenation of a prochiral pyrone. RajanBabu and co-workers[31] have recently reported that 3,5-dimethyl substitution can improve the ee's in the Rh-catalyzed hydrogenation of dehydroamino acids using the chelating ligands shown below.

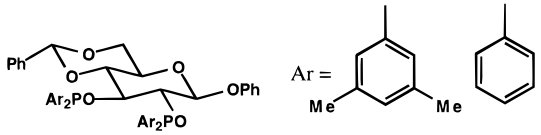


ee = 97-99% 62-94%

For four different substrates, they found that the observed ee was 5%, 6%,12%, and in one case 35% better than with the parent chelate. Recently, 3,5-dimethyl substitution has been shown to afford a good ee in the Ir-catalyzed hydrogenation of prochiral imines using the chiral ferrocene phosphine **9**.[32] Empirically, it seems that there is a "3,5-dialkyl meta-

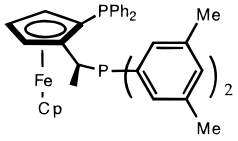


**9**

effect" on the observed enantioselectivity. This effect can be sizeable, ca. 14%, as in the Heck reaction noted above; however, it is more often modest in magnitude, perhaps only ca. 5−10%. In terms of energy, the observed Δee's correspond to only ca. 2−4 kJ/mol in $\Delta\Delta G^{\ddagger}$.

(31) RajanBabu, T. V.; Ayers, T. A.; Casalnuovo, A. L. *J. Am. Chem. Soc.* **1994**, *116*, 4101.

(32) Cited in Togni, A. *Chimia* **1996**, *50*, 87. Also cited in *Chem. Eng. News* **1996**, July, *22*, 38.

The Pd complex **5** and the Ru complex **6** show restricted rotation about several P−C bonds. Moreover, there are indications that a similar restricted rotation is observable in an Ir(III) complex of **9**.[33] Our MM3* calculations on the 3,5-di-*tert*-butyl-MeO−BIPHEP complex **6** suggest that the restricted rotations are to be expected and that the entire chiral array is increasingly rigid, relative to the parent complex. Freezing one or more rings results in a more selective chiral pocket, in agreement with our earlier calculations.[14a] It is only necessary for the $\Delta\Delta G^{\ddagger}$ to "remember" a fraction of the calculated energy differences to rationalize the observed improved ee's, relative to the parent complex.

On the basis of these various results with the Pd, Ru, Rh, and Ir complexes, we suggest that the observed dialkyl meta-effect on enantioselectivity is the combined result of a more rigid and slightly larger chiral pocket. This effect will have some generality in enantioselective homogeneous catalysis and may be useful in chiral ligand design.

It is worth remembering that the chiral pocket for any given auxiliary, be it a MeO−BIPHEP, a ferrocene type,[17,18] or a sugar-based diarylphosphinite,[31,34] will interact differently with coordinated ligands of varying size. Consequently, the extent of this 3,5-dialkyl meta-effect is expected to be substrate dependent. Further, enantioselective catalysis in which electronic effects combine with steric effects, e.g., hydrocyanation,[34] could well lead to an insignificant dialkyl meta-effect, so that each reaction will require individual consideration.

## Experimental Section

**General Procedures.** All reactions were performed in an atmosphere of Ar using standard Schlenk techniques. Dry and oxygen free solvents were used. $Ru(OAc)_2$(**1a**) (**2**) was provided by F. Hoffman-La Roche, Basel. Routine $^1$H (300.13 MHz) and $^{31}$P (121.5 MHz) NMR spectra were recorded with a Bruker DPX-300 spectrometer. Chemical shifts are given in parts per million, and coupling constants (*J*) are given in hertz. The two-dimensional studies were carried out at 500 MHz for $^1$H. NOESY measurements were carried out as reported previously.[14a,15] The $^{31}$P,$^1$H-correlation experiments were carried out at low temperature. The ROESY spectrum for **6** was measured twice at 193 K (500 MHz, $CD_2Cl_2$), with a 0.4 s spinlock. The carrier frequency was set in the middle of the proton spectrum in the first measurement and at ca. −5 ppm in the second. IR spectra were recorded with a Perkin-Elmer 882 infrared spectrophotometer. Elemental analyses and mass spectroscopic studies were performed at ETHZ.

**Crystallography.** A suitable crystal, mounted on a glass fiber, was cooled to 180 K by using an Enraf-Nonius FR558SH nitrogen gas-stream cryostat installed on a CAD4 diffractometer, which was used for the space group determination and for the data collection. Unit cell dimensions were obtained by least squares fit of the $2\theta$ values of 25 high-order reflections ($9.55 \leq \theta \leq 18.09°$). Selected crystallographic and other relevant data are listed in Table 3 and Supporting Information S1.

Data were measured with variable scan speed to ensure constant statistical precision on the collected intensities. Three standard reflections were used to check the stability of the crystal and of the experimental conditions and measured every 90 min; no significant variation was detected. Data were corrected for Lorentz and polarization factors using the data reduction programs of the MOLEN crystallographic package.[35] An empirical absorption correction was also applied (azimuthal ($\Psi$) scans of two reflections having $\chi > 88°$).[36] The standard deviations on intensities were calculated in terms of statistics alone, while those on $F_o$ were calculated as shown in Table 3.

The structure was solved by a combination of direct and Fourier methods and refined by full-matrix least squares. During the refinement, a Fourier difference map revealed the presence of a clathrated solvent molecule (THF), which was included in the refinement. Anisotropic displacement parameters were used for the heavy atoms, the cymene moiety, the ring substituents, and the solvent molecule; all other atoms were refined isotropically. Increasing the number of parameters, while giving an unfavorable observation to parameters ratio, did not yield a significantly better model.[37] As can be judged from the large displacement parameters of some atoms, two of the *tert*-butyl groups are disordered even though no model for it could be constructed.

It proved impossible to locate the hydride ligand on the difference Fourier maps; however, its position was unambiguously located by using the energy minimization program HYDEX[38] and successfully refined using an isotropic temperature factor. The function minimized was $[\sum_w(|F_o| - 1/k|F_c|)^2])$ with $w = [\sigma^2(F_o)]^{-1}$. No extinction correction was deemed necessary. The scattering factors used, corrected for the real and imaginary parts of the anomalous dispersion, were taken from the literature.[39] The handedness of the structure was tested by refining both enantiomorphs; the coordinates giving the significantly[37] lower $R_w$ factor were used. Upon convergence the final Fourier difference map showed no significant peaks. All calculations were carried out by using the Enraf-Nonius MOLEN crystallographic programs.[35]

**Calculations.** The MacroModel system as described by Still and co-workers[40] was used for the calculations on the MeO−BIPHEP complexes. The force field used was MM3*. Missing constants were added and optimized by hand to fit the experimental structure. The values used may be found as part of the Supporting Information together with one sample structure in MacroModel format. Monte Carlo techniques were used for the conformational analysis.

Barriers to the rotation of the phenyl rings were carried out with the angle driver technique supplied by MacroModel. All coordinates, except the driven dihedral angle, were optimized at each step.

**Dynamics Calculations.** The activation energies for the solution dynamics were determined using the method of Bain et al.[41] The calculated values of $50.0 \pm 0.9$ ($\gamma$), $42.4 \pm 2.7$ ($\alpha$), and $36.2 \pm 2.0$ ($\delta$) are associated with correlation coefficients of 0.994, 0.997, and 0.987, respectively. These activation energies were obtained with difficulty due to the complexity of the proton spectra, i.e., eight different environments, with similar chemical shifts, often overlapping.

**Preparation of [Pd($\eta^3$-PhCHCHCHPh)(1)]$PF_6$ (5).** [Pd($\eta^3$-PhCHCHCHPh)($\mu$-Cl)]$_2$ (33.5 mg, 50 $\mu$mol) was dissolved in 7 mL of acetone by gentle warming. $TlPF_6$ (35 mg, 0.1 mmol) was added and the precipitated TlCl filtered through Celite after 10 min. A solution of (*S*)-**1** (104 mg, 1 mmol) in $CH_2Cl_2$ was added. Evaporation to dryness and recrystallization of the residue from $CH_2Cl_2$/pentane gave the product as a yellow crystalline solid. Yield: 114 mg, 73 $\mu$mol, 73% of **5**·$CH_2Cl_2$. Anal. Calcd for $C_{85}H_{109}O_2F_6P_3Pd\cdot CH_2Cl_2$ (1561.1): C, 66.2; H, 7.17. Found: C, 66.5; H, 7.05. FAB-MS: *m/e* 1329.4 ($M^+ - PF_6$), 1136.3 [Pd(**1**)].

**Allylic Alkylation.** The procedure applied for the allylic alkylation was the same as described by Pfaltz et al.[8,10] Complex **5** was used as the catalyst precursor. The product was purified by column chromatography (silicagel F60, hexane−ethyl acetate, 65:35) The yield of the (+)-(R)-product was 70%. Anal. Calcd for $C_{20}H_{20}O_4$ (324.4): C, 74.06; H, 6.21. Found: C, 74.26; H, 6.07. EI-MS: *m/e* 324.2 ($M^+$). $^1$H-NMR ($CDCl_3$): $\delta$ 3.53 (s, 3H), 3.71 (s, 3H), 3.96 (d, $J = 10.9$ Hz, 1H), 4.27 (dd, $J = 8.4$, 10.9 Hz, 1H), 6.33 (dd, $J = 8.4$, 15.8 Hz, 1H) 6.49 (d, $J = 15.8$ Hz, 1H), 7.20−7.35 (m, $10H^{ar}$). HPLC: OD-H (Chiralcel, Daicel), UV-detector 254 nm, hexane−*i*-PrOH, 99:1, flow 0.5 mL/min; 90.5% ee, (+)-(*R*)-product; $t_R = 24.5$ min, $t_S = 26.9$ min.

(33) H. Rüegger, ETH Zentrum, Zürich, unpublished results.
(34) RajanBabu, T. V.; Casalnuovo, A. L. *J. Am. Chem. Soc.* **1996**, *118*, 6325.
(35) *MOLEN*, Enraf-Nonius Structure Determination Package; Enraf-Nonius: Delft, The Netherlands, 1990.
(36) North, A. C. T.; Phillips, D. C.; Mathews, F. S. *Acta Crystallogr., Sect. A* **1968**, *24*, 351.
(37) Hamilton , W. C. *Acta Crystallogr.* **1965**, *17*, 502.
(38) Orpen, A. G. *J. Chem. Soc., Dalton Trans.* **1980**, 2509.
(39) *International Tables for X-ray Crystallography*; Kynoch: Birmingham, England, 1974; Vol. IV.
(40) F. Mohamadi, F.; Richards, N. J. F.; Guida, W. C.; Liskamp, R. Lipton, M.; Caufield, C.; Chang, G.; Hendrickson, T.; Still, W. C. *J. Comput. Chem.* **1990**, *11*, 440.
(41) Bain, A. D.; Duns G. J. *J. Magn. Reson.* **1995**, *112A*, 258.

**Heck Reaction (Arylation of 2,3-Dihydrofuran with Phenyl Iodide or Phenyl Triflate). Procedure a.** $PdCl_2$(**1**) (18.1 mg, 15 $\mu$mol, 3 mol %) and $Ag_2CO_3$ (138 mg, 0.5 mmol, 2 equiv) were suspended in 5 mL of DMF in an ampule with a magnetic stirring bar. $C_6H_5I$ (102 mg, 0.5 mmol) and 2,3-dihydrofuran (105 mg, 1.5 mmol) were added and the ampule was sealed. The mixture was stirred over 7 d at 50 °C. The reaction mixture was added to 250 mL of pentane with stirring and the resulting suspension filtered. The solution was washed with water, dried over $MgSO_4$, and concentrated in vacuo. The crude products were separated and purified via column chromatography (silica gel F60, hexane−ethyl acetate, 98:2). (+)-(*S*)-2-Phenyl-2,3-dihydrofuran: $R_f$ = 0.4, **4a**. (−)-(S)-2-Phenyl-2,5-dihydrofuran: $R_f$ = 0.15, **4b**. The NMR data for **4a** and **4b** were consistent with those of the the literature. Results for the catalytic runs are given in the table below.

**Procedure[6,8] b1.** (S)-(**1**) (61.9 mg, 60 $\mu$mol, 6 mol %) and $Pd_2(dba)_3$ (14.9 mg, 30 $\mu$mol {Pd}, 3 mol %) were solved in 5 mL of THF, placed in an ampule with a magnetic stirring bar, and stirred at 60 °C for 20 min. The resulting homogeneous orange solution was cooled to room temperature and then treated with 2,3-dihydrofuran (377.8 $\mu$L, 5 mmol, 5 equiv), phenyl triflate (157 $\mu$L, 1 mmol), and *N*,*N*-diisopropylethylamine (510 $\mu$L, 3 mmol, 3 equiv). The ampule was closed and the mixture stirred at 70 °C for 7 d. The reaction mixture was worked up as described above. A second experiment, b2, was run with benzene as solvent.

**Procedure[6] c.** (S)-(**1**) (61.9 mg, 60 $\mu$mol, 6 mol %) and $Pd(OAc)_2$ (6.7 mg, 30 $\mu$mol, 3 mol %) were placed in an ampule with a magnetic stirring bar. This mixture was treated with 3 mL of benzene and 2,3-dihydrofuran (377.8 $\mu$L, 5 mmol, 5 equiv), and then stirred for 20 min. Phenyl triflate (157 $\mu$L, 1 mmol) and *N*,*N*-diisopropylethylamine (510 $\mu$L, 3 mmol, 3 equiv) were added, and the ampule was sealed. The reaction mixture was stirred at 40 °C for 7 d. The products were isolated as described above.

The absolute configuration was determined by the optical rotation of the products in comparison with the literature. Optical yields were measured by both $^1$H-NMR ($CDCl_3$) with the use of the optically active chemical shift reagent tris[3-((heptafluoropropyl)hydroxymethylene)-camphorato]europium(III) [Eu(hfc)$_3$] and HPLC (OD-H (Chiralcel, Daicel), UV-detector 258 and 225 nm, hexane−*i*-PrOH, 99.5:0.5, flow 0.5 mL/min; 2-phenyl-2,3-dihydrofuran; $t_R$ = 11.7 min, $t_S$ = 12.7 min).

| procedure | (*S*)-2-phenyl-2,3-dihydrofuran yield (optical purity) | (*S*)-2-phenyl-2,5-dihydrofuran yield (optical purity) |
|---|---|---|
| a | 17.4% (73% ee) | 13.8% (22% ee) |
| b1 | 34% (>98% ee) | 3% (>98% ee) |
| b2 | 44% (>98% ee) | 2% (>98% ee) |
| c | 65−70% (>98% ee) | 3% (>98% ee) |

**Preparation of [RuH(*p*-cymene)(1)]$BF_4$ (6).** This complex was originally prepared starting from $Ru(OAc)_2$(**1**) (68.4 mg, 0.0547 mmol), in 1 mL of 2-propanol. Addition of 2.1 equiv of $HBF_4$·$H_2O$ (14 $\mu$L of a 8.2 M solution in water, 0.11 mmol) was followed by 1.2 equiv (10 $\mu$L, 0.066 mmol) of *p*-cymene. The reaction mixture was then heated until refluxing started. After cooling to room temperature, the argon atmosphere was replaced by an atmosphere of $H_2$ (ca. 1.2 atm). The solution was heated again until it started to reflux. The pale yellow solution then stood overnight at room temperature under an atmosphere of $H_2$. After being transferred to a Schlenk tube the reaction mixture was taken to dryness in vacuo, and the residue washed twice with 3 mL of hexane and then redissolved in 4 mL of $CH_2Cl_2$. The resulting solution was extracted twice with 4 mL of $H_2O$, to remove inorganics, and the $CH_2Cl_2$ dried over $MgSO_4$. After filtration and drying in vacuo, removal of solvent affords the analytically pure product as a yellow powder in 81% yield. MS (FAB): *m/e* (found) 1267.8 ($M^+$). IR (KBr): 2030 cm$^{-1}$ (Ru−H; w), 1125−1045 cm$^{-1}$ ($BF_4^-$; s, br). Selected NMR data: $^{31}$P{$^1$H}-NMR ($CD_2Cl_2$, 193 K): $\delta$ 54.0, 52.6, $^2J$(P,P) = 46. $^1$H-NMR (500 MHz, $CD_2Cl_2$): −9.80 (hydride); 7.95, (3H), 7.61, 6.82, 6.71, 6.61, 6.06 (the eight *ortho* protons in Figure 2b); 3.12, 2.97 (2 OMe). Anal. Calcd for C, 70.94; H, 8.26. Found: C, 70.19; H, 8.26.

**Alternative Preparation of 6.** It is determined that hydrogen gas is not necessary for the preparation of **6.** The solvent is a sufficient source of the hydride ligand. To a solution of [Ru((*R*)−**1**)$(OAc)_2$] (14.0 mg, 0.0112 mmol) in 1 mL of 2-propanol in a NMR tube was added 5.7 equiv (10 $\mu$L, 0.064 mmol) of *p*-cymene followed by the addition of 2.0 equiv (2.7 $\mu$L of a 8.2 M solution in water, 0.022 mmol) of $HBF_4$·$H_2O$. After being transferred to a Schlenk vessel, the reaction mixture was taken to dryness in vacuo. The residue was washed twice with 2 mL of hexane and redissolved in 4 mL of $CH_2Cl_2$. Subsequently the solution was extracted twice with 2 mL of $H_2O$ and dried over $MgSO_4$. After filtration and drying in vacuo, the product was obtained as a yellow powder in 78% yield.

**Acknowledgment.** It is our pleasure to dedicate this paper to Professor Dieter Seebach on the occasion of his 60th birthday. P.S.P. thanks the Swiss National Science Foundation, the ETH Zurich, and F. Hoffmann-La Roche Ltd. for financial support. A.A. thanks MURST for partial support. We also thank F. Hoffmann-La Roche Ltd. for a gift of BIPHEP ligands and the complex $Ru(OAc)_2$(**1**), as well as Johnson Matthey for the loan of precious metals. Special thanks go to Dr. Renzo Salzmann for measuring several of the early NMR spectra on the 1,3-diphenylallyl complex.

**Supporting Information Available:** Tables of bond lengths and angles, complete atomic coordinates, anisotropic displacement coefficients, and isotropic displacement coefficients for hydrogen atoms, ORTEP plot with a full numbering scheme, and force field parameters added to mm3.fld and sample structure in MacroModel format for MM3* calculations (23 pages). See any current masthead page for ordering and Internet access instructions.

JA964406G